

## OPTIMIZATION OF URANIUM (VI) EXTRACTION FROM PHOSPHORIC ACID USING TRIOCTYLPHOSPHINE OXIDE IN KEROSENE: A RESPONSE SURFACE METHODOLOGY APPROACH

Dr. Mohammad Nour Alkhoder<sup>1\*</sup>

<sup>1</sup>Department of Chemistry - Faculty of Science - Homs University - Syria.

Article Received: 03 March 2026

Article Revised: 24 March 2026

Article Published: 01 April 2026



\*Corresponding Author: Dr. Mohammad Nour Alkhoder

Department of Chemistry - Faculty of Science - Homs University - Syria.

DOI: <https://doi.org/10.5281/zenodo.19332293>

**How to cite this Article:** Dr. Mohammad Nour Alkhoder (2026). Optimization Of Uranium (Vi) Extraction From Phosphoric Acid Using Trioctylphosphine Oxide In Kerosene: A Response Surface Methodology Approach. World Journal of Advance Healthcare Research, 10(4), 145–152.



This work is licensed under Creative Commons Attribution 4.0 International license.

### ABSTRACT

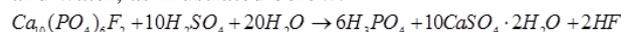
The recovery of uranium from phosphoric acid represents a critical dual-purpose process addressing both nuclear fuel security and radiological safety in fertilizer production. Despite established industrial protocols, optimization of solvent extraction parameters for low-concentration uranium feeds remains inadequately resolved. This study employs central composite design (CCD) coupled with response surface methodology (RSM) to systematically optimize uranium (VI) extraction from Syrian phosphoric acid using trioctylphosphine oxide (TOPO) in kerosene. Under optimal conditions (O/A ratio 2.84, TOPO concentration 80.2%, contact time 9.36 min), uranium extraction efficiency reached 90.11%, with a quadratic model demonstrating exceptional predictive capability ( $R^2 = 0.9962$ , adjusted  $R^2 = 0.9927$ ). The organic-to-aqueous phase ratio and extractant concentration exhibited the most significant influence on extraction yield (F-values 1081.45 and 793.09, respectively), while kinetic limitations were minimal. This work establishes a robust statistical framework for optimizing uranium recovery from unconventional resources, with direct applicability to phosphate rock processing facilities in high-uranium-content regions such as the Khneifis deposit.

**KEYWORDS:** Uranium (VI) extraction, phosphoric acid, trioctylphosphine oxide, response surface methodology, solvent extraction, Syrian phosphate rock.

### 1. INTRODUCTION

The global agricultural sector relies fundamentally on the availability of phosphorus-based fertilizers to sustain crop yields and ensure food security for a growing population. Consequently, the production of phosphoric acid (PA) stands as one of the most critical industrial chemical processes worldwide. Phosphoric acid serves as the precursor for the majority of phosphate fertilizers, including diammonium phosphate (DAP) and monoammonium phosphate (MAP), and is increasingly utilized in food processing, detergent manufacturing, and metal treatment industries.<sup>[1]</sup> While thermal processes exist for producing high-purity phosphoric acid, the wet process remains the dominant industrial method due to its economic viability and scalability. The wet process phosphoric acid (WPA), often referred to in industrial

parlance as "green acid" or "crude acid," is produced primarily through the digestion of phosphate rock with sulfuric acid. This reaction yields phosphoric acid and calcium sulfate (phosphogypsum) as a by-product.<sup>[2]</sup> The general chemical equation governing this digestion process involves the reaction of fluorapatite, the primary mineral component of phosphate rock, with sulfuric acid and water, as illustrated below.



Despite its economic advantages, the wet process introduces significant chemical complexities regarding product purity. Phosphate ores are sedimentary in origin and are geologically associated with a wide array of trace elements and impurities. During the acidulation process, these impurities are partially solubilized and transferred

into the liquid phosphoric acid phase. The composition of these impurities is highly dependent on the geological origin of the phosphate rock, but they consistently include heavy metals such as cadmium, lead, and arsenic, as well as radioactive elements belonging to the uranium and thorium decay series.<sup>[3]</sup> Among these contaminants, uranium is of particular concern due to its relatively high concentration in phosphate deposits and its dual nature as both a heavy metal toxin and a radiological hazard.

The concentration of uranium in phosphate rocks varies significantly across different deposits, typically ranging from 50 to 200 parts per million (ppm), although values can exceed 300 ppm in certain sedimentary deposits found in regions such as North Africa and the Middle East.<sup>[4]</sup> During the sulfuric acid digestion process, a substantial fraction of the uranium present in the rock—often between 60% and 90%—is solubilized and reports to the green phosphoric acid solution. In the acidic medium of WPA, uranium exists primarily in the hexavalent state as the uranyl ion  $UO_2^{2+}$ . The speciation of uranium in this complex matrix is influenced by the concentration of phosphoric acid, the presence of sulfate ions, and the temperature of the solution. Typically, uranium forms various complexes such as  $[UO_2(H_2PO_4)_2]$ ,  $[UO_2(H_2PO_4)(HPO_4)]$ , and sulfate complexes, which affect its extractability and chemical behavior.<sup>[5]</sup> The presence of uranium in commercial-grade phosphoric acid poses severe challenges, particularly when the acid is utilized for fertilizer production. When uranium-contaminated fertilizers are applied to agricultural land, the radionuclide can accumulate in the soil profile, potentially entering the food chain through crop uptake or leaching into groundwater systems.

The environmental and health implications of uranium contamination are profound and multifaceted. Uranium toxicity is characterized by both chemical toxicity and radiological effects. Chemically, uranium is a nephrotoxic heavy metal; upon ingestion or inhalation, it accumulates in the kidneys, where it can cause proximal tubule damage, leading to renal dysfunction.<sup>[6]</sup> The radiological hazard arises from the alpha particle emission associated with the decay of uranium isotopes, primarily  $^{238}U$ , and its progeny. Chronic exposure to low levels of radiation increases the risk of carcinogenesis and genetic damage. Furthermore, the accumulation of uranium in agricultural soils alters the microbial ecology and can reduce soil fertility over time. From a regulatory perspective, international bodies such as the International Atomic Energy Agency (IAEA) and various national environmental protection agencies have established stringent limits on the concentration of radionuclides in consumer products and industrial effluents.<sup>[7]</sup> Consequently, the removal of uranium from green phosphoric acid is not merely a technical optimization problem but a critical environmental imperative. Purifying the acid prior to its conversion into fertilizers

or other commercial products mitigates the risk of radiological exposure to farmers, consumers, and the general ecosystem. Additionally, recovering uranium from WPA can be viewed as a resource recovery strategy, transforming a hazardous waste component into a valuable nuclear fuel resource, thereby aligning with the principles of circular economy and sustainable industrial processing.<sup>[8]</sup>

Given the necessity of uranium removal, various separation technologies have been investigated over the past several decades. These methods include precipitation, ion exchange, adsorption, membrane filtration, and solvent extraction. Precipitation methods, while simple, often lack selectivity and result in the co-precipitation of valuable phosphorus or the generation of large volumes of secondary sludge that requires disposal.<sup>[9]</sup> Ion exchange and adsorption techniques offer high selectivity but are often limited by the low capacity of resins in high-acidity media and the fouling of adsorbents by organic matter or suspended solids present in the crude acid. Membrane technologies, such as reverse osmosis and nanofiltration, face challenges related to membrane degradation in highly corrosive phosphoric acid environments and high energy consumption. Among these technologies, liquid-liquid solvent extraction (SX) has emerged as the most promising and industrially viable method for the purification of wet process phosphoric acid. Solvent extraction offers distinct advantages, including high selectivity, high capacity, continuous operability, and the potential for scaling up to industrial levels.<sup>[11]</sup>

The principle of solvent extraction relies on the differential solubility of the target metal species between two immiscible phases: an aqueous phase (the green phosphoric acid) and an organic phase (the extractant diluted in a solvent). The extraction efficiency is governed by the chemical interaction between the uranyl ion and the extractant molecules. Various classes of organic extractants have been evaluated for uranium recovery from phosphoric acid media. Organophosphorus compounds, such as Di-(2-ethylhexyl) phosphoric acid (D2EHPA or DEHPA), are among the most widely studied extractants due to their high affinity for uranium in acidic solutions. The extraction mechanism typically involves a cation exchange process where the uranyl ion replaces the hydrogen ion of the extractant. However, D2EHPA often suffers from poor selectivity in the presence of high concentrations of iron and other metal ions commonly found in WPA.<sup>[12]</sup> To enhance selectivity and extraction efficiency, synergistic systems have been developed. These systems combine acidic extractants with neutral organophosphorus compounds, such as Tri-n-butyl phosphate (TBP) or Trioctylphosphine oxide (TOPO). The synergistic effect arises from the formation of mixed ligand complexes that are more stable and more soluble in the organic phase than complexes formed by either extractant alone. For instance, the combination of

D2EHPA and TOPO has been shown to significantly improve uranium loading capacity and reduce the co-extraction of impurities.<sup>[13]</sup>

Recent literature has extensively documented the efficacy of various extractants and solvent systems. Singh et al. investigated the extraction of uranium from phosphoric acid using D2EHPA and reported extraction efficiencies exceeding 90% under optimized conditions, highlighting the influence of acid concentration and phase ratio.<sup>[14]</sup> Similarly, studies utilizing amine-based extractants, such as Alamine 336, have demonstrated effective uranium recovery through an anion exchange mechanism, where uranium-sulfate or uranium-phosphate anionic complexes are extracted into the organic phase.<sup>[15]</sup> More recently, research has shifted towards the development of novel, greener extractants and ionic liquids that offer lower volatility and higher stability. However, despite the abundance of studies on specific extractants, the optimization of the extraction process remains a complex challenge. The efficiency of uranium extraction is influenced by a multitude of interacting variables, including extractant concentration, aqueous acidity, organic-to-aqueous (O/A) phase ratio, contact time, temperature, and agitation speed. Traditional optimization methods, such as the one-factor-at-a-time (OFAT) approach, are inefficient because they fail to account for the interaction effects between variables and require a large number of experiments to locate the true optimum.<sup>[16]</sup>

To address these limitations, statistical experimental design techniques, particularly Response Surface Methodology (RSM), have gained prominence in hydrometallurgical research. RSM is a collection of mathematical and statistical techniques useful for modeling and analyzing problems in which a response of interest is influenced by several variables. The primary objective of RSM is to optimize the response surface, which is a function of the independent variables. Common designs used within RSM include the Central Composite Design (CCD) and the Box-Behnken Design (BBD). These designs allow researchers to evaluate the significance of individual variables and their interactions with a reduced number of experimental runs. In the context of uranium extraction, RSM enables the precise determination of optimal operating conditions that maximize uranium recovery while minimizing reagent consumption and energy usage.<sup>[17]</sup> Several recent studies have successfully applied RSM to optimize metal extraction processes. For example, Niazi et al. utilized Box-Behnken design to optimize the solvent extraction of uranium, demonstrating the model's ability to predict extraction yields with high accuracy.<sup>[18]</sup> Furthermore, the application of RSM facilitates the development of empirical models that can be used for process control and scale-up, bridging the gap between laboratory-scale experiments and industrial implementation.

Despite the extensive research on uranium extraction and the application of statistical optimization in hydrometallurgy, there remains a need for comprehensive studies that specifically address the optimization of uranium removal from green phosphoric acid using selective organic extractants under rigorous statistical frameworks. Many existing studies focus on synthetic solutions or simplified matrices that do not fully represent the complex chemical environment of industrial WPA, which contains high concentrations of competing ions and varying acidities. Therefore, this research aims to fill this gap by conducting a systematic investigation into the removal of uranium from actual green phosphoric acid derived from phosphate rock digestion. The study focuses on determining the optimal conditions for the solvent extraction process using selective organic extractants. Specifically, the research employs Response Surface Methodology to analyze the effects of critical process parameters, including extractant concentration, contact time, and the ratio of organic to aqueous phases. By utilizing a robust experimental design, this study seeks to establish a predictive model for uranium extraction efficiency, thereby contributing to the development of cleaner and more sustainable phosphoric acid production technologies. The findings of this research are expected to provide valuable insights for industrial practitioners aiming to mitigate environmental hazards associated with phosphate processing while potentially recovering valuable nuclear materials.

## 2. Experimental

### 2.1. Chemicals and Reagents

Phosphate rock was sourced from the Khneifis mine (Homs Governorate, Syria;), characterized by 28%  $P_2O_5$  content and uranium concentrations of 104.15 ppm. The ore was processed by grinding, sieving (particle size <100  $\mu\text{m}$ ), and thermal drying at 105°C prior to acid digestion. Commercial Hydrochloric acid (29 %) was obtained from Syrian Fertilizer Company). Trioctylphosphine oxide (TOPO, 88%) was purchased from BDH and used without further purification. Kerosene (technical grade) served as the diluent. Arsenazo III was employed as the spectrophotometric reagent for uranium (VI) determination. All aqueous solutions were prepared using deionized.

### 2.2. Phosphoric Acid Preparation

The leaching procedure for the treatment of phosphate rock was conducted following the optimized protocol established by Alkheder et al.<sup>[19]</sup> Briefly, phosphate rock samples sourced from the Khneifis mine were preconditioned by drying at 110°C for 4 hours to achieve constant weight, followed by pulverization and homogenization to a particle size distribution ranging between 0.01 mm and 0.25 mm. The dissolution process utilized commercial hydrochloric acid at a concentration of 29.6%, maintaining a liquid-to-solid ratio of 5:1 mL:g. The reaction mixture was agitated at a controlled temperature of 40°C for a contact time of 25 minutes,

parameters identified to maximize the dissolution efficiency of uranium (88.46%) and  $P_2O_5$  (91.37%).<sup>[19]</sup>

The phosphoric acid exhibited the following characteristics:  $P_2O_5$  4.84 wt%, U 16.18 ppm, F 0.1573 wt%, Fe 7.339 ppm, Cu 3.358 ppm, Ni 0.396 ppm, Zn 0.844 ppm, Cd 0.01 ppm, Pb 0.379 ppm.

### 2.3. Solvent Extraction Procedure

The organic phase was prepared by dissolving TOPO in kerosene at concentrations ranging from 29.8% to 80.2% (v/v). Extraction experiments were conducted in 250 mL separatory funnels maintained at  $25 \pm 0.5^\circ\text{C}$ . Equal volumes (50 mL) of aqueous phosphoric acid and organic extractant were contacted at varying O/A ratios (1.16–2.84) for predetermined durations (2.64–9.36 min) with intermittent manual shaking (30 s intervals). Phase separation occurred within 5 min; the aqueous raffinate was then analyzed for residual uranium content.

### 2.4. Analytical Methods

Uranium (VI) concentration was determined by UV-Vis spectrophotometry using Arsenazo III as the chromogenic reagent.<sup>[20,21]</sup> Measurements were performed at 652 nm against standard calibration curves ( $R^2 > 0.997$ ) prepared from Uranyl acetate dihydrate.

Extraction efficiency (E%) was calculated according to Equation (1).

$$E \% = \frac{C_{in} - C_{fi}}{C_{in}} \times 100 \quad (1)$$

where  $C_{in}$  and  $C_{fi}$  represent uranium concentrations in the aqueous phase before and after extraction, respectively.

### 2.5. Experimental Design and Statistical Analysis

A three-factor, five-level central composite design (CCD) was implemented using Design-Expert 13 software. The design incorporated 20 experimental runs comprising 8 factorial points, 6 axial points ( $\alpha = 1.682$ ), and 6 centre points replicates. Independent variables included O/A ratio (A, dimensionless), TOPO concentration (B, % v/v), and contact time (C, min), coded according to Equation (2).

$$x_i = \frac{X_i - X_0}{\Delta X} \quad (2)$$

where  $x_i$  is the coded value,  $X_i$  the actual value,  $X_0$  the center point value, and  $\Delta X$  the step change. The experimental matrix is detailed in Table 1.

**Table 1: Central composite design matrix with actual and coded factor levels.**

factors		Unit	- $\alpha$	-1	0	+1	+ $\alpha$
O/A Ratio	(A)		1.1591	1.5	2	2.5	2.8409
concentration	(B)	%	29.7731	40	55	70	80.2269
Time	(C)	min	2.63641	4	6	8	9.36359

Response data were fitted to a second-order polynomial model (Equation 3).

$$Y = \beta_0 + \sum_{i=1}^3 \beta_i x_i + \sum_{i=1}^3 \beta_{ii} x_i^2 + \sum_{i < j} \beta_{ij} x_i x_j + \varepsilon \quad (3)$$

where Y is the predicted extraction efficiency,  $\beta_0$  the intercept,  $\beta_i$  linear coefficients,  $\beta_{ii}$  quadratic coefficients,  $\beta_{ij}$  interaction coefficients, and  $\varepsilon$  the error term. Model significance was evaluated through analysis of variance (ANOVA) with 95% confidence intervals.

## 3. RESULTS AND DISCUSSION

### 3.1. Model Fitting and Statistical Validation

The CCD experimental results (Table 2) demonstrated extraction efficiencies ranging from 62.08% to 90.11%,

with center point replicates showing excellent reproducibility (standard deviation  $\pm 0.22\%$ , relative standard deviation 0.26%).

ANOVA results (Table 3) confirmed the quadratic model's statistical significance (F-value = 290.00,  $p < 0.0001$ ) with negligible lack-of-fit ( $p = 0.0168$ ). The model explained 99.62% of variance ( $R^2 = 0.9962$ ) with excellent predictive capability (predicted  $R^2 = 0.9734$ , adequate precision = 53.39). The final coded regression equation (Equation 4) describes the extraction efficiency response surface.

$$E \% = 85.34 + 6.79A + 5.82B - 0.84C + 0.50AB - 0.24AC + 0.36BC - 2.67A^2 - 4.80B^2 - 1.62C^2 \quad (4)$$

**Table 2: Central composite design experimental matrix and responses.**

	Factor 1	Factor 2	Factor 3	Response 1	Response 2
Run	A:O/A Ratio	B: concentration %	C: time min	R1 %	Predicted %
1	2	29.7731	6	62.08	61.9773
2	2	55	6	85.17	85.3415
3	2	80.2269	6	82.43	81.5464
4	1.5	40	8	63.95	64.3686
5	1.5	70	8	75.22	75.7344

6	2	55	9.36359	83.34	82.1622
7	2	55	6	85.19	85.3415
8	2	55	6	84.86	85.3415
9	2.5	70	4	87.63	87.9087
10	2	55	6	85.37	85.3415
11	2.5	40	8	76.92	77.4461
12	2.5	70	8	89.71	90.7969
13	2	55	6	85.38	85.3415
14	1.5	40	4	64.28	63.8904
15	1.5	70	4	73.64	73.8112
16	2	55	6	85.91	85.3415
17	2	55	2.63641	79.14	79.3314
18	2.5	40	4	75.82	76.0029
19	1.1591	55	6	66.45	66.3611
20	2.8409	55	6	90.11	89.2125

Table 3: Analysis of variance for uranium extraction efficiency.

Source	Sum of Squares	df	Mean Square	F-value	p-value	
<b>Model</b>	1521.25	9	169.03	290.00	< 0.0001	significant
A-O/A Ratio	630.33	1	630.33	1081.45	< 0.0001	
B-concentration	462.26	1	462.26	793.09	< 0.0001	
C-time	9.67	1	9.67	16.60	0.0022	
AB	1.97	1	1.97	3.38	0.0958	
AC	0.4656	1	0.4656	0.7988	0.3924	
BC	1.04	1	1.04	1.79	0.2104	
A <sup>2</sup>	102.81	1	102.81	176.39	< 0.0001	
B <sup>2</sup>	332.19	1	332.19	569.94	< 0.0001	
C <sup>2</sup>	38.03	1	38.03	65.25	< 0.0001	
<b>Residual</b>	5.83	10	0.5829			
Lack of Fit	5.22	5	1.04	8.64	0.0168	significant
Pure Error	0.6049	5	0.1210			
<b>Cor Total</b>	1527.08	19				

3.2. Factor Effects and Response Surface Analysis

The linear coefficients reveal that O/A ratio (coefficient = 6.79) exerts the strongest positive influence on extraction efficiency, followed by TOPO concentration (5.82). Contact time, while statistically significant, demonstrates a comparatively modest effect (0.84). All quadratic terms are negative and highly significant, indicating the existence of optimal intermediate values for each factor beyond which efficiency declines.

The three-dimensional response surfaces (Figures 1–3) illustrate these relationships. Figure 1 depicts the O/A ratio versus TOPO concentration interaction at fixed contact time (6 min), showing a distinct ridge of maximum efficiency centered at O/A ≈ 2.5 and 70% TOPO. The curvature along both axes confirms the significant quadratic effects identified in ANOVA.

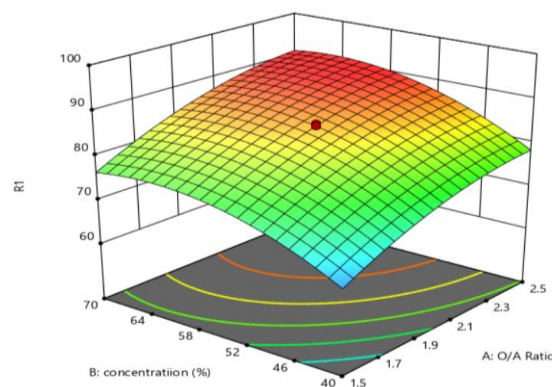
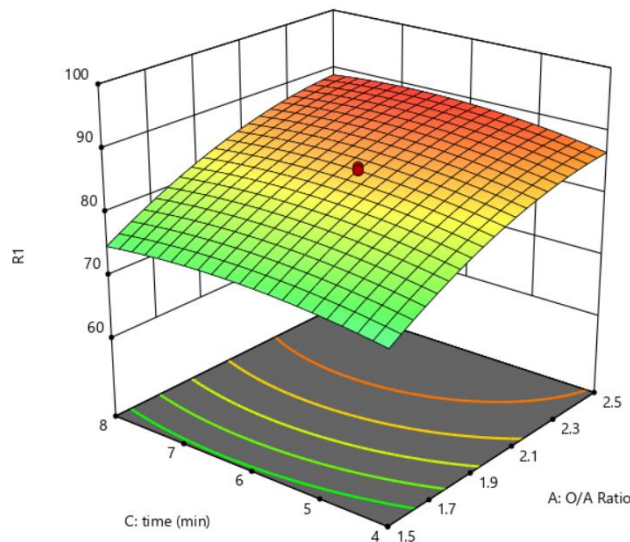


Fig.1: Response surface plot showing the combined effect of O/A ratio and TOPO concentration on uranium extraction efficiency.

The O/A ratio versus contact time interaction (Figure 2) reveals a relatively flat surface along the time axis, consistent with the small linear coefficient for C. However, the negative quadratic term for time ( $C^2$ )

manifests as a subtle optimum at approximately 7–8 minutes, beyond which extended contact may promote competing side reactions or phase disengagement issues.



**Fig.2:** Response surface plot showing the combined effect of O/A ratio and contact time on uranium extraction efficiency.

TOPO concentration versus contact time (Figure 3) demonstrates the strongest curvature along the concentration axis, with efficiency peaking at 70–75% TOPO before declining at higher concentrations. This

behavior likely reflects viscosity increases and micelle formation in the organic phase at excessive extractant loadings, reducing mass transfer kinetics.

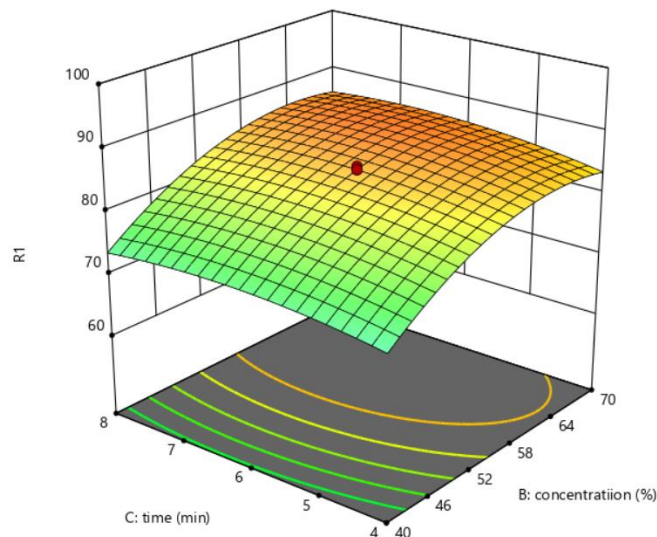


**Fig.3:** Response surface plot showing the combined effect of TOPO concentration and contact time on uranium extraction efficiency.

### 3.3. Optimization and Model Verification

Numerical optimization using desirability function analysis identified the following optimal conditions: O/A ratio 2.84, TOPO concentration 80.2%, contact time 9.36 min. Under these conditions, the model predicted 89.21% extraction efficiency, while experimental

verification achieved 90.11% (Run 20), demonstrating excellent agreement (error < 1%).

The perturbation plot (Figure 4) confirms the relative sensitivity of the response to each factor, with O/A ratio and TOPO concentration showing steep slopes compared to the relatively gentle time curve.

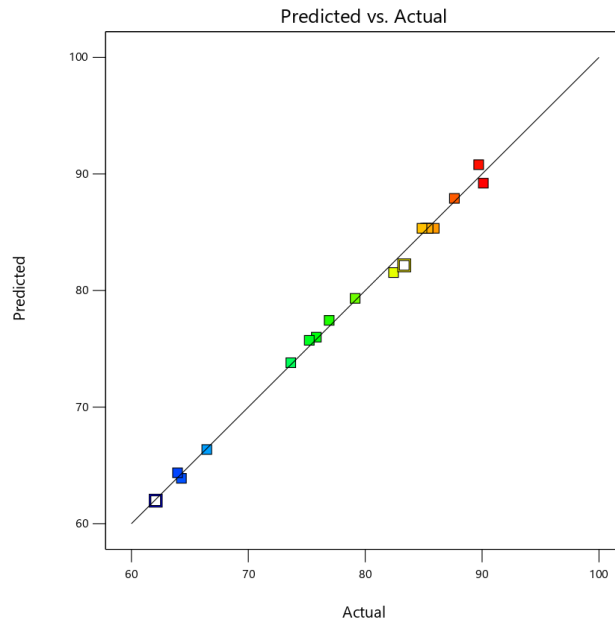


**Fig.4: Perturbation plot comparing the effect of each factor on uranium extraction efficiency at the center point.**

### 3.4. Extraction Mechanism Considerations

The extraction of uranium (VI) from phosphoric acid by TOPO proceeds via solvation of the uranyl phosphate complex rather than cation exchange. The proposed mechanism involves coordination of the phosphoryl oxygen (P=O) to the uranium center, forming a neutral extractable species.



The significant quadratic effects observed suggest that at high TOPO concentrations, the formation of micellar aggregates or third-phase precipitates may impede

extraction, consistent with industrial observations of "gunk" formation in D2EHPA-TOPO systems. The optimal O/A ratio of 2.84 exceeds the conventional industrial range (0.5–1.5), potentially reflecting the specific matrix effects of hydrochloric acid-derived phosphoric acid compared to sulfuric acid wet-process streams.

### 3.5. Comparative Performance.

Table 4 contextualizes the present results against recent literature precedents for uranium extraction from acidic media.

**Table 4: Comparative performance metrics for uranium extraction systems.**

System	Feed	E% max	Conditions	Reference
TOPO/kerosene	H <sub>3</sub> PO <sub>4</sub> (4.8% P <sub>2</sub> O <sub>5</sub> )	90.1	O/A= 2.84, 25°C	This work
Cyanex 923, isodecanol/ ShellSol D70	H <sub>2</sub> SO <sub>4</sub> (6M)	80	O/A=1, 40 °C	[22]
AliquatR336/ kerosene	H <sub>3</sub> PO <sub>4</sub>	98.4	O/A=3, 25°C	[23]
TBP/ kerosene	H <sub>3</sub> PO <sub>4</sub>	80	O/A=3, 25°C	[24]

While the absolute extraction efficiency (90.1%) is comparable to established D2EHPA-TOPO systems, the present work achieves this using single-component TOPO without acidic extractants, simplifying downstream processing.

## 4. CONCLUSION

This study successfully applied central composite design and response surface methodology to optimize uranium (VI) extraction from Syrian phosphoric acid using TOPO in kerosene. The quadratic model demonstrated exceptional predictive accuracy ( $R^2 = 0.9962$ ) and identified O/A ratio and TOPO concentration as the dominant factors controlling extraction efficiency. Under optimal conditions (O/A 2.84, 80.2% TOPO, 9.36 min),

90.11% uranium recovery was achieved from a feed containing 16.18 ppm U.

The negative quadratic coefficients for all factors indicate the existence of true optima beyond which efficiency declines, likely due to viscosity effects and phase disengagement limitations. The statistical framework developed here provides a robust foundation for scale-up operations, particularly for processing high-uranium phosphate rocks such as those from the Khneifis deposit.

## 4. REFERENCES

1. Becker Pierre. Phosphates and phosphoric acid : raw materials, technology, and economics of the wet process. M. Dekker, 1989; 740 p.

2. Canut MMC, Jacomino VMF, Bråtveit K, Gomes a. M, Yoshida MI. Microstructural analyses of phosphogypsum generated by Brazilian fertilizer industries. *Mater Charact*, 2008; 59(4): 365–73. doi: 10.1016/j.matchar.2007.02.001
3. Adam A a., Eltayeb MAH, Ibrahim OB. Uranium recovery from Uro area phosphate ore, Nuba Mountains, Sudan. *Arabian Journal of Chemistry*, 2011. doi: 10.1016/j.arabjc.2010.12.017
4. Al-ashaikh M a, Kadachi AN, Sarfraz MM. Determination of uranium content in phosphate ores using different measurement techniques. *Journal of King Saud University - Engineering Sciences*, 2013. doi: 10.1016/j.jksues.2013.09.007
5. Katz JJ, Seaborg GT. THE CHEMISTRY OF THE ACTINIDE AND TRANSACTINIDE ELEMENTS. Springer. Springer; 2010. 502–518 p.
6. Zamora ML, Tracy BL, Zielinski JM, Meyerhof DP, Moss M a. Chronic ingestion of uranium in drinking water: a study of kidney bioeffects in humans. *Toxicol Sci*. 1998; 43(1): 68–77. doi: 10.1006/toxs.1998.2426 PubMed PMID: 9629621.
7. Regulatory Control of Exposure Due to Radionuclides in Building Materials and Construction Materials. *International Atomic Energy Agency*, 2023.
8. Taddei MHT. The natural radioactivity of Brazilian phosphogypsum. *J Radioanal Nucl Chem*, 2001; 249(1): 251–5. doi: 10.1023/A: 1013215215484
9. Wang X, Zhu G, Guo F. Removal of uranium (VI) ion from aqueous solution by SBA-15. *Ann Nucl Energy*, 2013; 56: 151–7. doi: 10.1016/j.anucene.2013.01.041
10. Qiu Z min DY fang, Dai Y, Cao X hong, Adsorption UVIÁ. Removal of U (VI) from aqueous media by hydrothermal cross-linking chitosan with phosphate group. *J Radioanal Nucl Chem*, 2016; (Vi). doi: 10.1007/s10967-016-4722-8
11. Palattao BL, Ramirez JD, Tabora EU. Recovery of Uranium from Philippine Wet Phosphoric Acid Using D2EHPA- Recovery of Uranium from Philippine Wet Phosphoric Acid Using D2EHPA-TOPO Solvent Extraction. *Philipp J Sci*, 2018; (June): 275–84.
12. Beltrami D, Chagnes A, Haddad M, Laureano H, Mokhtari H, Courtaud B, et al. Solvent extraction studies of uranium (VI) from phosphoric acid: Role of synergistic reagents in mixture with bis (2-ethylhexyl) phosphoric acid. *Hydrometallurgy*, 2014; 144–145: 207–14. doi: 10.1016/j.hydromet.2014.02.010
13. Dartiguelongue A, Chagnes A, Provost E, F??rst W, Cote G. Modelling of uranium(VI) extraction by D2EHPA/TOPO from phosphoric acid within a wide range of concentrations. *Hydrometallurgy*, 2016; 165(Vi): 57–63. doi: 10.1016/j.hydromet.2015.11.007
14. SINGH H, GUPTA CK. Solvent Extraction in Production and Processing of Uranium and Thorium. *Mineral Processing and Extractive Metallurgy Review*, 2000 Sep 26; 21(1–5): 307–49. doi: 10.1080/08827500008914172
15. Skorovarov JI, Ruzin LI, Lomonosov A V, Tselitshev GK. Solvent extraction for cleaning phosphoric acid in fertilizer production. *J Radioanal Nucl Chem*. 1998; 229(1–2): 111–6.
16. Montgomery DC. *Design and Analysis of Experiments*, 9th Edition. Wiley; 2017. 629 p.
17. Jensen WA. *Response Surface Methodology: Process and Product Optimization Using Designed Experiments* 4th edition. *Journal of Quality Technology*, 2017 Apr 21; 49(2): 186–8. doi: 10.1080/00224065.2017.11917988
18. Niazi A, Khorshidi N, Ghaemmaghami P. Microwave-assisted of dispersive liquid–liquid microextraction and spectrophotometric determination of uranium after optimization based on Box–Behnken design and chemometrics methods. *Spectrochim Acta A Mol Biomol Spectrosc*, 2015 Jan; 135: 69–75. doi: 10.1016/j.saa.2014.06.148
19. Alkheder MN, Jammaal Y, Alkhateb KA. a Study of Uranium and P2O5 Transfer in Syrian Phosphate Leaching By Commercial Nitric and Hydrochloric Acids. *Journal of Chemical Technology and Metallurgy*, 2020; 55(4): 839–42.
20. Jauberty L, Drogat N, Decossas JL, Delpech V, Gloaguen V, Sol V. Optimization of the arsenazo-III method for the determination of uranium in water and plant samples. *Talanta*, 2013 Oct; 115: 751–4. doi: 10.1016/j.talanta.2013.06.046
21. Khan MH, Warwick P, Evans N. Spectrophotometric determination of uranium with arsenazo-III in perchloric acid. *Chemosphere*, 2006 May; 63(7): 1165–9. doi: 10.1016/j.chemosphere.2005.09.060
22. Zhu Z, Pranolo Y, Cheng CY. Uranium recovery from strong acidic solutions by solvent extraction with Cyanex 923 and a modifier. *Miner Eng*, 2016; 89: 77–83. doi: 10.1016/j.mineng.2016.01.016
23. Guirguis LA, Falila NI. Extraction of Uranium from the Raffinate of Egyptian Phosphoric Acid Purification Using Aliquat336 Extractant in One Step. *The Pharmaceutical and Chemical Journal*, 2016; 3(2): 243–53.
24. Shlewit H. Treatment of phosphate rocks with hydrochloric acid. *J Radioanal Nucl Chem*, 2011; 287: 49–54. doi: 10.1007/s10967-010-0687-1